Structural, elastic, electronic, and magnetic properties of Ni$_2$MnSb, Ni$_2$MnSn, and Ni$_2$MnSb$_{0.5}$Sn$_{0.5}$ magnetic shape memory alloys

O. Benguerine[a], Z. Nabi[a], B. Benichou[b,*], B. Bouabdallah[c], H. Bouchenafa[d], M. Maachou[a] and R. Ahuja[e]
[a]*Laboratory of Catalysis and Reactive Systems, Physics Department,*
Djillali Liabès University, Sidi Bel Abbès 22000, Algeria.
[b]*Department of Electronics, Faculty of Technology,*
Hassiba Benbouali University, Chlef 02000, Algeria.
[*]e-mail: boucif_benichou@yahoo.fr
[c]*Physics Department, Djillali Liabès University, Sidi Bel Abbès 22000, Algeria.*
[d]*Physics Department, Faculty of Sciences Exact and Informatics,*
Hassiba Benbouali University, Chlef 02000, Algeria.
[e]*Condensed Matter Theory Group, Department of physics and Astronomy,*
Uppsala University, Box 516, 75120, Uppsala, Sweden.

Structural, elastic, electronic, and magnetic properties of the Nickel-based magnetic shape memory alloys (MSMA) Ni2MnSb, Ni$_2$MnSn and Ni$_2$MnSb$_{0.5}$Sn$_{0.5}$, are investigated using the full-potential linearized plane wave plus local orbital method (FP-LAPW+lo). With Perdew-Burke-Ernzerhof (PBE) exchange-correlation, generalized gradient approximation (GGA) is used to describe the electronic exchange correlation energy. Equilibrium lattice constant, bulk modulus, and its pressure derivative are calculated and compared with available data. Using the total energy versus strain in the framework of the FP-LAPW+lo approach, we compute the elastic constants of the studied compounds in their austenite structure. Good agreement is found with other calculations both for Ni$_2$MnSb and Ni$_2$MnSn. Magnetic moments agree well with available results.

Keywords: Ab initio study; MSMA alloys; elastic constants; quaternary Heusler alloy.

1. Introduction

Recently, tremendous experimental and theoretical interest arose for Ni-based Heusler alloys because of two unique properties that they exhibit: shape memory effect and inverse magneto caloric effect. Indeed, due to their extraordinary magneto-elastic properties as actuators and sensors [1-3], magnetic shape memory alloys (MSMA) are good candidates for future technological applications. A MSMA, Ni$_2$MnGa has been studied extensively [4-8]. Despite its outstanding properties, Ni$_2$MnGa has a relatively low Curie and martensitic transformation temperature, high brittleness, its Gallium constituent expensive, etc. Nevertheless, Ni$_2$MnSb and Ni$_2$MnSn alloys with composition close to stoichiometric Heusler structure are promising ferromagnetic MSMA [9,10]. This is due to the fact that Ni$_2$MnSn and Ni$_2$MnSb alloys have martensitic transformation domain close to room temperature, a requirement for technological applications. Full Heusler quaternary alloys of the type X$_2$Y$_{1-x}$Y$_x$Z, X$_2$YZ$_{1-x}$Z$_x$ and (X$_{1-x}$X$_x$)$_2$YZ have been extensively studied. Galanakis studied a series of Heusler alloys (Co$_2$[Cr$_{1-x}$M$_x$]Al, Co$_2$Mn[Al$_{1-x}$Sn$_x$], and [Fe$_{1-x}$Co$_2$]MnAl) [11]. Ahmadian *et al.* investigated the bulk Co$_2$Ti$_{1-x}$Fe$_x$Ga Heusler alloys and Co$_2$Ti$_{0.5}$Fe$_{0.5}$Ga (001) surfaces, electronic and magnetic properties [12]. Some first-principles electronic structure calculations have been done on Ni$_2$MnX (X=Sn, Sb) systems, with the idea

of realizing new MSMA's with better performances than that of Ni$_2$MnGa. Most of the calculations were focused on these alloys compressibilities [13]. Hydrostatic effect on Curie's temperature (TC) has been experimentally studied with pressure [10]. Gavrillunk performed Ni$_2$MnSn isothermal compressibility and Mossbauer high-pressure experiment [14]. Şaşioğlu *et al.* investigated Ni$_{(1−x)}$MnSb system exchange interactions and Curie's temperature [15]. Very recently, Benichou *et al.* [16] have studied the electronic structure, elastic, and magnetic properties of quaternary Heusler alloy Cu$_2$MnSn$_{1-x}$In$_x$ ($x = 0$, 0.25, 0.5, 0.75, 1) using an ab-initio calculation by substituting the main group element (Sn by In) in this compound. The Cu$_2$MnSn$_{1-x}$In$_x$ alloy is found to be ferromagnetic, metallic compound, brittle, and anisotropic in nature.

The aim of this paper is to provide a detailed study of the structural, elastic, electronic, and magnetic properties for Nickel based Heusler compounds and to study Ni$_2$MnSb$_{0.5}$Sn$_{0.5}$ quaternary alloy. In Sec. 2, we outline our computational procedure. The results are discussed in Sec. 3 and summarized in Sec. 4.

2. Computational procedure

Using spin polarized density functional theory (DFT) [17,18] with full potential linear augmented plane wave plus local orbitals (FP-LAPW+lo) method as implemented in the

TABLE I. Calculated values for the lattice parameter (a), bulk modulus (B) and its pressure derivative (B') for Ni_2MnSb, Ni_2MnSn, and $Ni_2MnSb_{0.5}Sn_{0.5}$ compounds.

Compounds		a(Å)	B(GPa)	B'
Ni_2MnSb	NM	5.9384	179.6488	5.2373
	FM 6.0515	137.226	5.2916	
		6.00 [13]	168.3 [13]	6.00 [13]
		6.004 [23]	139.7 [25]	
		6.051 [25]		
Ni_2MnSn	NM	5.9433	185.2524	4.2997
	FM	6.0426	145.7315	4.7048
		5.92 [13]	168.5 [13]	2.9 [13]
		6.053 [23]	140 [24]	4.89 [25]
		6.068 [25]	138.4 [25]	
		6.06 [28]	146.38 [28]	
$Ni_2MnSb_{0.5}Sn_{0.5}$	NM	5.9712	216.0407	6.0765
	FM	6.0798	168.9919	5.3129

WIEN2k code [19], we determine total energy and electronic structure. Perdew-Burke-Ernzerhof generalized gradient approximation (PBE-GGA) [20] is used to get the exchange correlation potential. Wave functions are expanded up to angular momentum $l_{max} = 10$ inside the muffin-tin spheres. The G_{max} parameter was taken to be 12.0. Convergence parameter $R_{MT}*K_{MAX}$ is set to 7.0. R_{MT} is the smallest MT radius and K_{MAX} is the magnitude of the largest K vector in plane wave expansion. Ni, Mn, Sb, and Sn atoms radii are set to 2.2, 2.0, 1.9 and 1.9 a.u. (atomic units), respectively. Total and partial densities of states are calculated by tetrahedral integration method [21]. The self-consistent calculations were considered to be convergent when the total energy was stable within 0.1 mRy. Mesh of 104 and 4 special Brillouin zone (BZ) k-points were used in the irreducible wedge of the BZ for the parent ternary and quaternary compounds, respectively. The cut-off energy was chosen to be -8 Ry. The full-Heusler alloys have cubic $L2_1$ (Cu$_2$MnAl-type) structure with the space group Fm-3m-225. The lattice contains four

interpenetrating fcc sublattices at positions (0,0,0) for Mn, (1/4,1/4,1/4), (3/4,3/4,3/4) for Ni and (1/2,1/2,1/2) for Z (Z = Sb, Sn). In order to simulate $Ni_2MnSbSn$ quaternary alloy, a Ni_2MnSb original unit cell was extended to an eight-atoms supercell by substituting one Sb atom by one Sn atom. This corresponds to 0.5 doping concentration for both Sb and Sn atoms.

3.   Results and discussion

3.1.   Structural and elastic properties

Ni_2MnSb, Ni_2MnSn, and $Ni_2MnSb_{0.5}Sn_{0.5}$ compounds structural properties are calculated. Total energy variation with volume was fitted to the Murnaghan equation of state [22] to obtain the equilibrium lattice constant and bulk modulus. Results are listed in Table I along with the available theoretical and experimental data. Good agreement is found
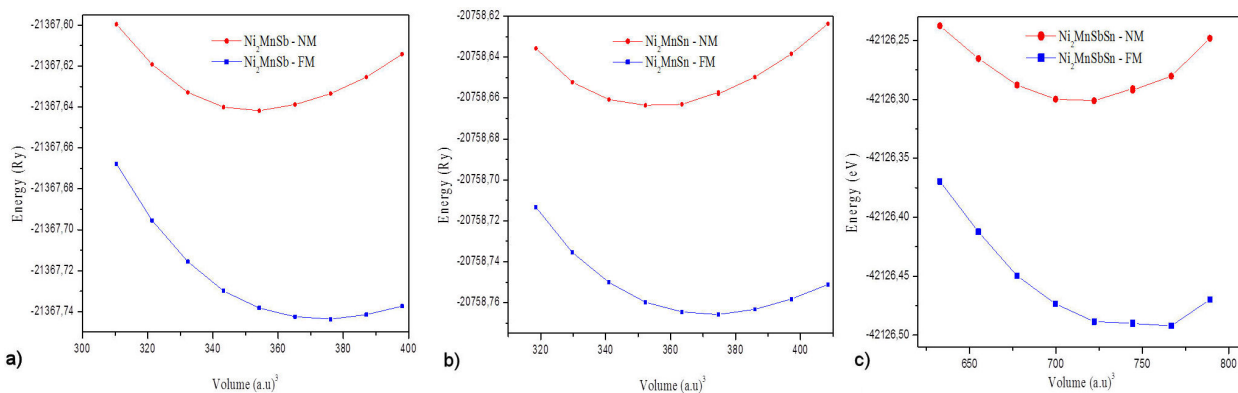
FIGURE 1. Variation of calculated total energy as a function of lattice constant for Ni_2MnSb, Ni_2MnSn, and $Ni_2MnSb_{0.5}Sn_{0.5}$ compounds for both non-magnetic and ferromagnetic phases.

TABLE II. Elastic constants in (GPa), bulk modulus (GPa), C' and A for Ni_2MnSb, Ni_2MnSn, and $Ni_2MnSb_{0.5}Sn_{0.5}$ compounds.

Compounds	C_{11}	C_{12}	C_{44}	B	C'	A
Ni_2MnSb	161.97	148.41	89.49	153.20	6.78	13.20
	143.7 [25]	137.7 [25]	74.924[25]		3.0 [25]	24.97[25]
Ni_2MnSn	168.76	140.23	78.32	150.00	14.26	5.49
	161.02[26]	128.5 [25]	87 [24]	145.31[26]	14.8 [25]	5.49 [25]
	158.1 [25]	137.46[26]	81.3 [25]	138.4 [25]	8 [24]	11 [24]
	158.12 [28]	128.41[28]	92.56 [26]			
			81.28 [28]			
$Ni_2MnSb_{0.5}Sn_{0.5}$	155.74	131.33	63.62	139.47	12.20	5.21
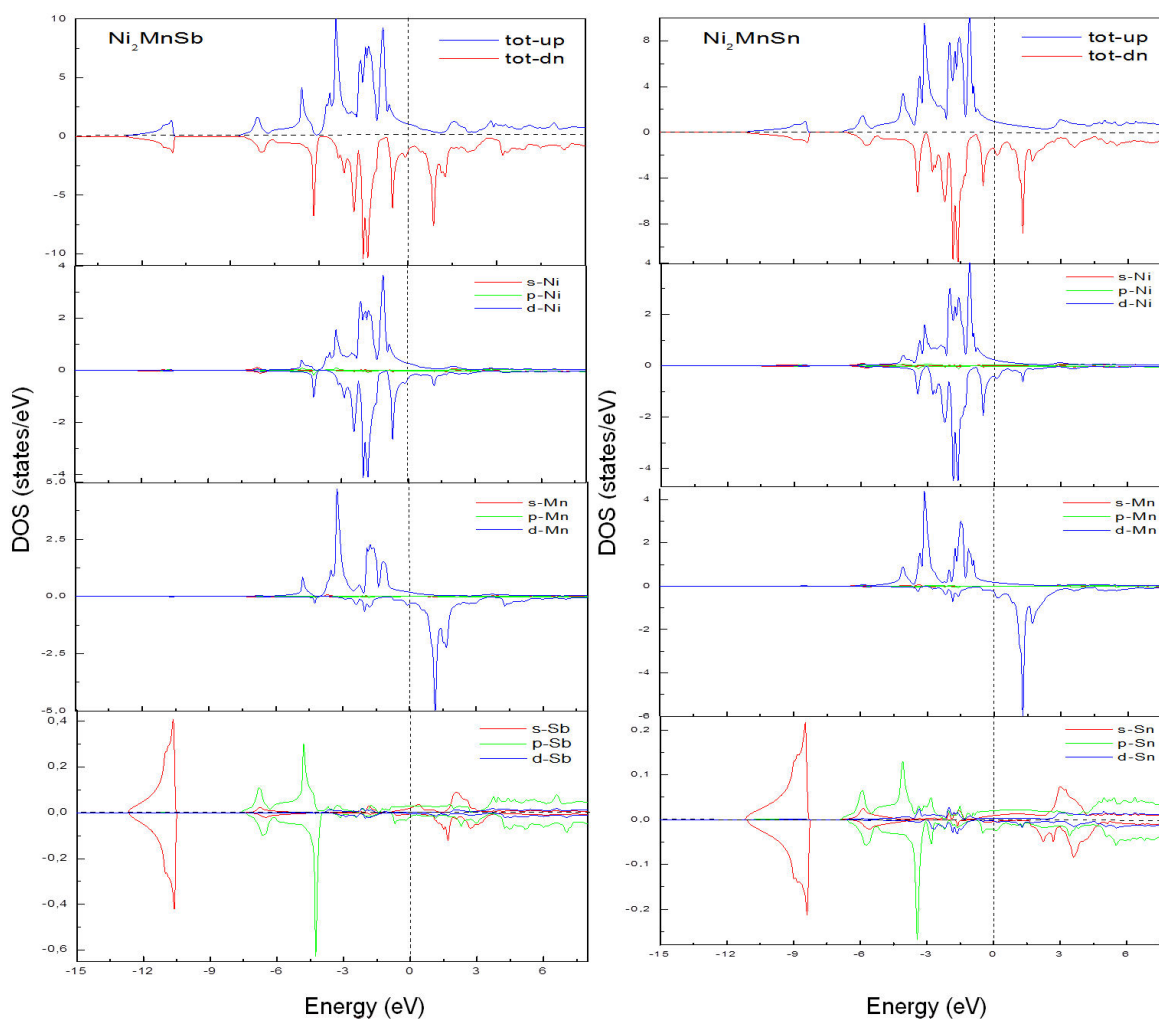
FIGURE 2. Spin-dependent total and partial density of states for Ni_2MnSb and Ni_2MnSn compounds.

theoretical and experimental data. Good agreement is found with the available data [13,23-28], with the exception of the quaternary alloy. Total energy under compression for all alloys is plotted in Fig. 1. The ferromagnetic state is found to be more stable than corresponding non-magnetic state for all materials presented.

To the best of our knowledge, there are no comparable studies about $Ni_2MnSbSn$ in the literature. So, we have estimated the lattice constant by utilizing the Vegard's law in Eq. (1),
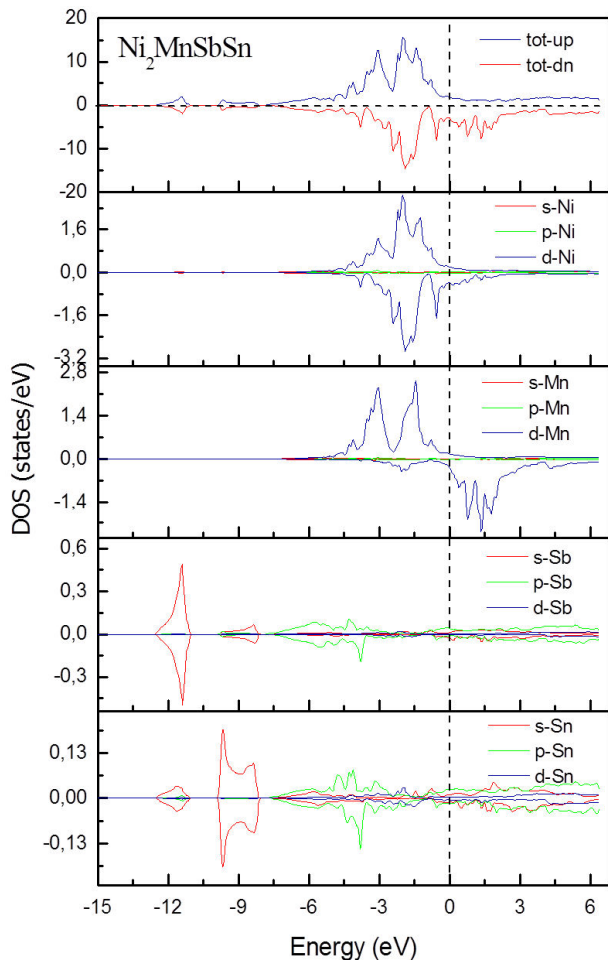
FIGURE 3. Spin-dependent total and partial density of states for Ni$_2$MnSb$_{0.5}$Sn$_{0.5}$ compound.

$$Ni_2MnSb_{1-x}Sn_x : a(\text{Å}) = 6.05 \times (1 - x) + 6.04 \times x,$$

$$Ni_2MnSb_{0.5}Sn_{0.5} : a(\text{Å}) = 6.05 \times 0.5 + 6.04 \times 0.5$$

$$= 6.04705. \quad (1)$$

Elastic constants for all three materials are computed at room pressure using the Charpin method, developed and integrated in WIEN2k [29]. Stability criteria for cubic crystals requires [30]:

$$C_{11} - C_{12} > 0, \quad C_{11} > 0, \quad C_{44} > 0,$$

$$C_{11} + 2C_{12} > 0, \quad C_{12} < B < C_{11}. \quad (2)$$

The three independent cubic crystal elastic constants are given in Table II. Bulk modulus, calculated from of elastic constants $B = (1/2)(C_{11} + C_{12})$ theoretical values are listed in Table II; it is nearly the same value as the one obtained from energy minimization. C_{11}, C_{12}, and C_{44} agree quite well with available theoretical results for Ni$_2$MnSb and Ni$_2$MnSn. However, due to experimental difficulties in preparing martensite single crystals, only few reliable complete sets of low symmetry martensite phases in MSMAs elastic constants are reported.

Concerning the stability criteria, we note that Eq. (2) is satisfied by Ni$_2$MnSb, Ni$_2$MnSn, and Ni$_2$MnSb$_{0.5}$Sn$_{0.5}$. Material stability is better described by two other parameters shown in Table II: Shear constant, defined as $C' = 1/2(C_{11} - C_{12})$ and elastic anisotropy ratio A, given by $A = C_{44}/C'$. The values of C' and A for all three studied compounds lie well within the limits observed in shape memory alloys MSMA [25,31-34]. No experimental or theoretical data for the elastic constants of the quaternary alloy Ni$_2$MnSb$_{0.5}$Sn$_{0.5}$ are available in scientific literature; therefore, we expect our results to provide baseline data for future investigations.

3.2. Electronic and magnetic properties

In their stable magnetic structure, Heusler compounds Ni$_2$MnSb and Ni$_2$MnSn total and partial density of states calculations are shown in Fig. 2.

Overall, band shapes in all couple of compounds are similar. It is also seen that both majority and minority bands cross the Fermi level in almost all high symmetry directions; thus, confirming a metallic ferromagnetic character. Like most Heusler alloys containing Ni$_2$MnGa, a pseudo-gap is formed below Fermi level. As for Ni$_2$MnGa, we see a double peak structure very close to Fermi level (Fig. 2). According to Barman *et al.* [35], this double peak plays a crucial role in favoring martensitic transition. Moreover, we note that the (-4.5 eV; $+3$ eV) bands for Ni$_2$MnSb (Ni$_2$MnSn) in both majority and minority spin states are mainly due to d states hybridization of Mn and Ni atoms. The (-12 eV; -10.5 eV) bands are caused by Sb (Sn) atoms s states, while (-7.5 eV; -4.5 eV) bands are due to Sb (Sn) atoms p states.

Figure 3 shows calculated Ni$_2$MnSb$_{0.5}$Sn$_{0.5}$ total and partial DOS. DOS shape has changed slightly from parent compounds. Peaks are very sharp. This quaternary alloy is metallic. Bands around -12 eV and -4 eV are due to Sn and Sb atoms s and p states. The energy range between -5 eV and $+2.5$ eV is governed by Ni and Mn atoms d states hybridization.

Calculated Heusler compounds Ni$_2$MnSb and Ni$_2$MnSn total and local magnetic moments are listed in Table III, together with available theoretical data [13,15,24,25,27,28].

In general, good agreement is found. In this work, calculated spin magnetic moment distribution shows that Ni$_2$MnSb and Ni$_2$MnSn are ferromagnetic with magnetic moment of Ni parallel to that of Mn, while a very small anti-aligned moment is observed for Sb and Sn atoms. Table III shows that the total magnetic moment, which includes the interstitial region contribution comes mainly from Mn atoms for both compounds (3.39 μB for both Ni$_2$MnSb and Ni$_2$MnSn). The robust Mn moment character results from the large exchange Mn $3d$ states splitting. It is important to notice that only one spin projection Mn $3d$ states (spin-up) are "strongly" occupied. The spin-down Mn $3d$ states main part lies above Fermi level. According to Şaşioğlu [36], who

TABLE III. Calculated total and local magnetic moments in (μB) for Ni_2MnSb, Ni_2MnSn, and $Ni_2MnSb_{0.5}Sn_{0.5}$ compounds.

Compounds	M^{Tot}	M^{Ni}	M^{Mn}	M^{Sn}	M^{Sb}
Ni_2MnSb	3.96	0.15	3.39	———	-0.00469
	3.94 [15]	0.14 [15]	3.69 [15]		
	3.87 [13]				
	4.12 [25]				
Ni_2MnSn	4.06	0.24	3.39	-0.0116	———
	3.86 [13]	0.24 [24]	3.53 [24]	-0.03 [24]	
	4.08 [24]	0.21 [28]	3.61 [28]		
	4.20 [25]				
	4.05 [27]				
	4.18 [28]				
$Ni_2MnSb_{0.5}Sn_{0.5}$	4.5	0.39	3.56	-0.016	0.0078

used Anderson $s - d$ mixing model [37], there is a variety of magnetic behavior in Mn-based Heusler alloys that can be interpreted in terms of competition between ferromagnetic RKKY-type exchange and antiferromagnetic superexchange. For $Ni_2MnSb_{0.5}Sn_{0.5}$, the total spin magnetic moment is calculated by integration over the entire cell. We notice that the total moment has increased from its parent compounds. Even for Mn and Ni spin moments, we observe a slight increase.

4. Conclusion

We investigated structural, elastic, electronic, and magnetic properties for Ni_2MnSb, Ni_2MnSn, and $Ni_2MnSb_{0.5}Sn_{0.5}$ alloys using (FP-LAPW+lo) method within GGA. Our results showed good agreement with available data. Elastic constants are numerically estimated and good agreement is found with other calculations. We predict that quaternary alloy $Ni_2MnSb_{0.5}Sn_{0.5}$ is likely a candidate for martensitic transformation. Thus, it seems possible to obtain alloys exhibiting martensitic transformation and possibly magnetically controlled shape memory effect by alloying in a small amount of Sb or Sn. We hope that our work proves to be useful for future experiments on spintronic field measurements, and provide a guide for experimentalists working in this field.

1. P. J. Webster, K. R. A. Ziebeck, S. L. Town, and M. S. Peak, *Phil. Mag. B.* **49** (1984) 295.

2. C. Biswas, R. Rawat, and S. R. Barman, *Appl. Phys. Lett.* **86** (2005) 202508.

3. A. Sozinov, A. A. Likhachev, N. Lanska, and K. Ullakko, *Appl. Phys. Lett.* **80** (2002) 1746.

4. M. E. Gruner, W. A. Adeagbo, A. T. Zayak, A. Hucht, S. Buschmann, and P. Entel, *Eur. Phys. J. Spec. Top.* **158** (2008) 193.

5. Q.-M. Hu, C.-M. Li, R. Yang, S. E. Kulkova, D. I. Bazhanov, B. Johansson, and L. Vitos, *Phys. Rev. B.* **79** (2009) 144112.

6. M. A. Uijttewal, T. Hickel, J. Neugebauer, M. E. Gruner, and P. Entel, *Phys. Rev. Lett.* **102** (2009) 035702.

7. V. D. Buchelnikov *et al.*, *J. Phys. D: Appl. Phys.* **44** (2011) 064012.

8. S. Ghosh, L. Vitos, and B. Sanyal, *Physica B* **406** (2011) 2240.

9. P. J. Webster and R.M. Mankikar, *J. Magn. Magn. Mater.* **42** (1984) 300.

10. T. Kanomata, K. Chirakawa, and T. Kaneko, *J. Magn. Magn. Mater.* **65** (1987) 76.

11. I. Galanakis, *J. Phys. Condens. Matter.* **6** (2004) 3089.

12. F. Ahmadian and A. Boochani, *Physica B* **406** (2011) 2865.

13. M. Pugaczowa-Michalska, *Acta Phys. Pol. A.* **113** (2008) 629.

14. A. G. Gavriliuk, G. N. Stepanov, V. A. Sidorov, and S. M. Irkaev, *J. Appl. Phys.* **79** (1996) 2609.

15. E. Şaşioğlu, L.M. Sandratskii, and P. Bruno, *J. Magn. Magn. Mat.* **385** (2005) 290.

16. B. Benichou, H. Bouchenafa, Z. Nabi, and B. Bouabdallah, *Rev. Mex. Fis.* **65** (2019) 468.

17. P. Hohenberg and W. Kohn, *Phys. Rev. B.* **136** (1964) 864.

18. W. Kohn and L. J. Sham, *Phys. Rev.* **140** (1965) A1133.

19. P. Blaha, K. Schwarz, G. K. H. Madsen, D. Kvasnicka, J. Luitz, R. Laskowski, F. Tran and L. D. Marks, *WIEN2k* (Techn. Universitaät Wien, Austria, 2018).

20. J. P. Perdew, K. Burke, and M. Ernzerhof, *Phys. Rev. Lett.* **77** (1996) 3865.

21. J. Rath and A. J. Freeman, *Phys. Rev. B.* **11** (1975) 2109.

22. F. D. Murnaghan, *Proc. Natl, Acad Sci. USA*. **30** (1944) 5390.

23. P. J. Webster and K. R. A. Ziebeck, in *Alloys and Compounds of d-Elements with Main Group Elements*, edited by H. P. J. Wijn (Springer, Heidelberg, 1988), Part 2, Vol. 19C, pp. 75-184.

24. A. Ayuela, J. Enkovaara, K. Ullakko, and R. M. Nieminen, *J. Phys. Condens. Matter*. **11** (1999) 2017.

25. S. Ağduk and G. Gökoğlu, *J. Alloys Compd.* **511** (2012) 9.

26. T. Roy, D. Pandey, and A. Chakrabarti, *Phys. Rev. B*. **93** (2016) 184102.

27. P. J. Webster, *Comtemp. Phys*. **10** (1969) 559.

28. B. Hamri, B. Abbar, A. Hamri, O. Baraka, A. Hallouche, and A. Zaoui, *Comput. Condens. Matter.* **3** (2015) 14.

29. P. Blaha, K. Schwarz, G. Madsen, and J. Luitz, User's guide. *WIEN2k Vienna University of Technology Austria* (2010).

30. G.V. Sin'ko, and N.A. Smirnov, *J. Phys. Condens. Matter*. **14** (2002) 6989.

31. K. Otsuka and X. Ren, *Prog. Mater. Sci.* **50** (2005) 511.

32. T. Černoch, M. Landa, P. Novák, P. Sedálk, and P. Šittner, *J. Alloys. Comp*. **378** (2004) 140.

33. S. M. Shapiro, G. Xu, G. Gu, J. Gardner, and R. W. Fonda, *Phys. Rev. B*. **73** (2006) 214114.

34. S. M. Shapiro, Guangyong Xu, B. L. Winn, D. L. Schlagel, T. Lograsso, and R. Erwin, *Phys. Rev. B*. **76** (2007) 054305.

35. S. R. Barman, S. Banik, and Aparna Chakrabati, *Phys. Rev. B.* **72** (2005) 184410.

36. E. Şaşioğlu, L. M. Sandratskii and P. Bruno, *Phys. Rev. B*. **77** (2008) 064417.

37. P. W. Anderson, *Phys. Rev*. **124** (1961) 41.